

THE FATE OF FALLBACK MATTER AROUND NEWLY BORN COMPACT OBJECTS

ROSALBA PERNA^{1,2}, PAUL DUFFELL³, MATTEO CANTIELLO⁴, ANDREW I. MACFADYEN³

¹JILA & Department of Astrophysical and Planetary Sciences, University of Colorado, 440 UCB, Boulder, CO80309-0440, USA;
rosalba@jilau1.colorado.edu

²Department of Physics and Astronomy, Stony Brook University, Stony Brook, NY 11794-3800, USA

³Center for Cosmology and Particle Physics, Department of Physics, New York University, 4 Washington Place, New York, NY 10003, USA and

⁴Kavli Institute for Theoretical Physics, University of California, Santa Barbara, Kohn Hall, CA 93106, USA

Draft version July 26, 2018

ABSTRACT

The presence of fallback disks around young neutron stars has been invoked over the years to explain a large variety of phenomena. Here we perform a numerical investigation of the formation of such disks during a supernova explosion, considering both neutron star (NS) and black hole (BH) remnants. Using the public code MESA, we compute the angular momentum distribution of the pre-supernova material, for stars with initial masses M in the range $13 - 40 M_{\odot}$, initial surface rotational velocities v_{surf} between 25% and 75% of the critical velocity, and for metallicities Z of 1%, 10% and 100% of the solar value. These pre SN models are exploded with energies E varying between $10^{50} - 3 \times 10^{52}$ ergs, and the amount of fallback material is computed. We find that, if magnetic torques play an important role in angular momentum transport, then fallback disks around NSs, even for low-metallicity main sequence stars, are *not* an outcome of SN explosions. Formation of such disks around young NSs can only happen under the condition of negligible magnetic torques and a fine-tuned explosion energy. For those stars which leave behind BH remnants, disk formation is ubiquitous if magnetic fields do not play a strong role; however, unlike the NS case, even with strong magnetic coupling in the interior, a disk can form in a large region of the Z, M, v_{surf}, E parameter space. Together with the compact, hyperaccreting fallback disks widely discussed in the literature, we identify regions in the above parameter space which lead to extended, long-lived disks around BHs. We find that the physical conditions in these disks may be conducive to planet formation, hence leading to the possible existence of planets orbiting black holes.

Subject headings: stars: evolution — stars: neutron — supernovae: general — accretion, accretion disks

1. INTRODUCTION

The presence of fallback associated with supernova (SN) explosions was recognized since early SN studies (Colgate 1971; Chevalier 1989). It occurs when part of the ejecta fails to achieve terminal escape velocity and accretes onto the central compact object. If some of this material has angular momentum larger than the keplerian value at the last stable orbit (or at the surface of the compact object, if a neutron star), then the formation of a disk is expected.

Fallback disks around newly born compact objects have been invoked to explain a large variety of phenomena. Hyperaccreting disks formed from the fallback of massive, rapidly rotating stars, whose iron cores collapse into black holes, are believed to provide the energy source that powers the class of long-duration Gamma-Ray Bursts (GRBs) (Woosley 1993, MacFadyen & Woosley 1999). MacFadyen & Woosley (1999) studied the formation and evolution of such a disk numerically, following the explosion of a $35 M_{\odot}$ main sequence star with angular momentum in the $3 \times 10^{16} - 2 \times 10^{17} \text{ cm}^2 \text{ s}^{-1}$ range. The detailed angular momentum structure of the fallback material is believed to play a role in the early X-ray emission following the prompt GRB (e.g. Kumar et al. 2008; Cannizzo & Gehrels 2009; Perna & MacFadyen 2010; Geng et al. 2013).

In the case of neutron stars (NSs), there is a much larger variety of phenomena that has been potentially ascribed to the presence of a fallback disk. Michel & Dessler (1981) and Michel (1988) originally emphasized that the presence of such disks can play a role in the evolution of young NSs. Lin, Woosley & Bodenheimer (1991) noticed how such disks can provide a clue regarding the formation of planets around

young neutron stars, while Chatterjee, Hernquist & Narayan (2000), and Alpar (2001) showed how fallback disks around NSs of ages $\sim 10^4 - 10^5$ yr can produce, by accretion onto the NS surface, X-ray luminosities as high as $\sim 10^{35} - 10^{36}$ erg/s. These are sufficient to explain the X-ray luminosities of the Anomalous X-ray Pulsars, a class of neutron stars whose X-ray luminosity is 1-2 orders of magnitudes higher than their spin down energy, at odds with the more traditional radio pulsars, whose X-ray emission is powered by their rotational energy loss. Fallback disks have also been invoked (Xu et al. 2003; Shi & Xu 2003) to explain the observational properties of the central compact objects (Pavlov et al. 2004) in supernova remnants.

The effects of fallback disks on the spin evolution of neutron stars have been discussed by a number of authors. Marsden, Lingenfelter & Rothschild (2001) pointed out how the interaction of a putative fallback disk with the magnetosphere of a NS can significantly modify its spin down rate, and as such help cure the discrepancy between the characteristic and the actual age that has been observed in some pulsars. Menou et al. (2001a; see also Chen & Li 2006; Yan et al. 2012) showed how the extra torque provided by this putative fallback disk can also result in braking indices which depart from the value of 3 expected for spin down by pure dipole radiation. Blackman & Perna (2004) further noticed that the presence of such a disk can play an important role for producing the jets that are observed in some of these pulsars, such as Crab and Vela. Qiao et al. (2003) proposed a fallback disk model for periodic timing variations of pulsars. Cordes & Shannon (2008) were able to explain the properties of the recently discovered transient pulsars by means of asteroids formed from a fallback disk and occasionally migrating into the pulsar light cylinder.

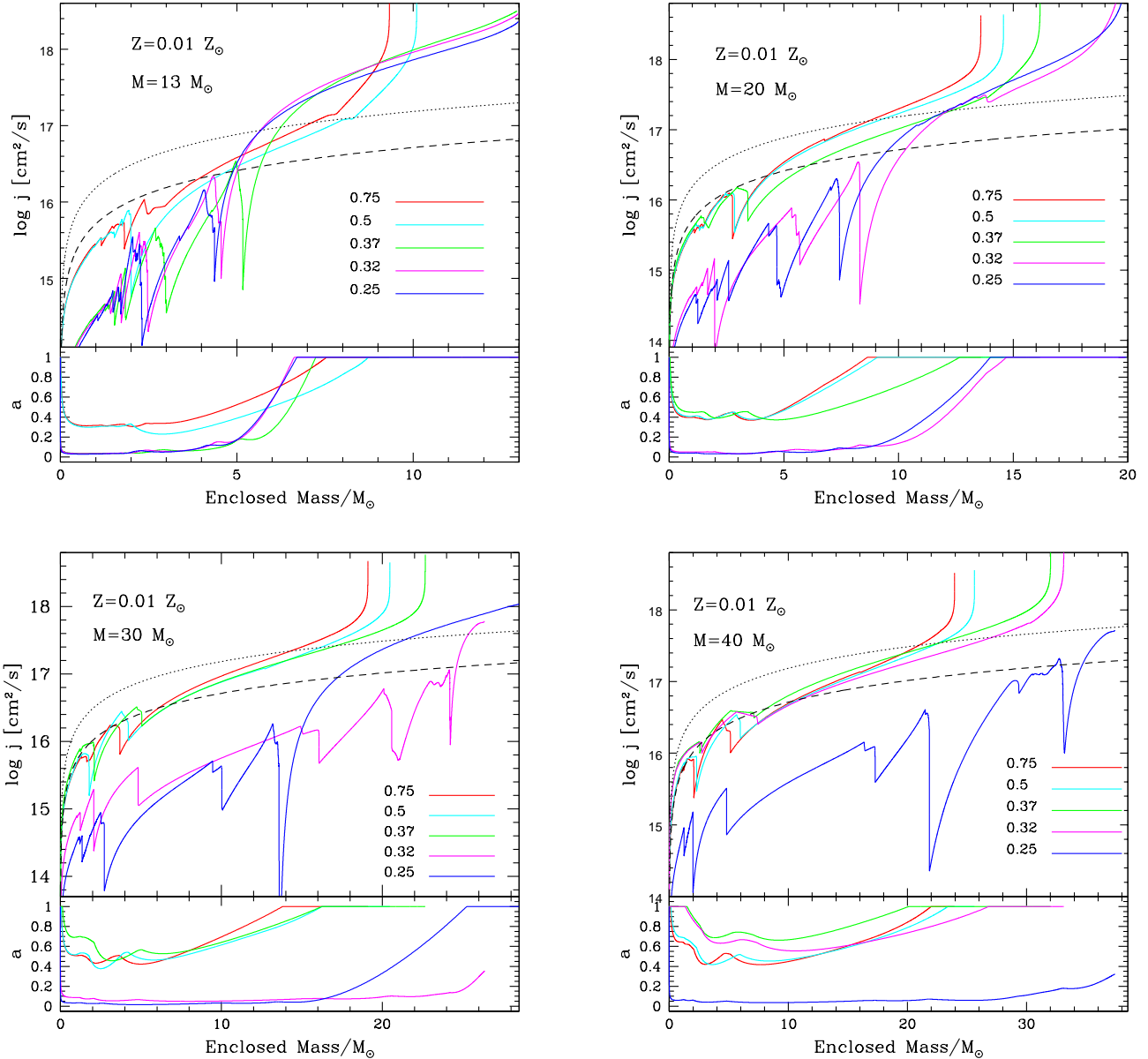


FIG. 1.— The distribution of specific angular momentum in the pre-SN star for main sequence stars of 1% solar metallicity and a range of initial surface rotational velocities, expressed in units of the critical velocity. Dashed and dotted lines in the upper region of each panel represent, respectively, the specific angular momentum of the last stable orbit around a Schwarzschild black hole and a maximally rotating Kerr black hole (of mass equal to the enclosed mass). The spin parameter of the enclosed material is shown, for each pre-SN model, in the bottom region of each panel.

The mass ejected by fallback in a supernova explosion has been invoked as a production site for the r-process (Fryer et al. 2006), as well as a potential source of power to SN light curves (Piro & Ott 2011; Dexter & Kasen 2013).

From an observational point of view, fallback disks around NSs of $10^4 - 10^5$ yr are expected to be especially bright in infrared radiation (Perna, Hernquist & Narayan 2000), and there have been many searches aimed at detecting such emission (see e.g. Mignani et al. 2007 for a review), resulting in some strong hints of possible detection (Wang, Chakrabarty & Kaplan 2006).

All the various models and scenarios discussed above, proposed to explain a large variety of astrophysical phenomena, especially in the context of the NS compact object remnants, depend crucially on the specific properties of the fall-

back disks. In particular they depend on the specific angular momentum content, which eventually determines the post-fallback circularization radius. Once fallback has ended, this initial radius, coupled with the local viscous timescale, will determine the initial accretion rate. After their formation, the evolution of fallback disks can be modeled following the results of semi-analytical and numerical studies (e.g. Cannizzo, Lee & Goodman 1990; Cannizzo & Gehrels 2009; Shen & Matzner 2013): an early phase of constant accretion rate, lasting on the order of the viscous time, followed by a powerlaw decay. Once the initial accretion rate \dot{M}_0 is known, then the subsequent evolution is determined in a self-similar fashion. Crucial, therefore, are the *initial conditions*, i.e. the mass and location of the matter that falls back and hence determines \dot{M}_0 . These can only be determined accurately by means of nu-

merical simulations of the collapse of massive rotating stars, and a distribution of angular momenta.

Numerical simulations of pre-SN profiles in stars with a range of masses and metallicities have been performed by a number of authors (e.g. Woosley & Weaver 1995; Fryer & Heger 2000; MacFadyen, Woosley & Heger 2001; Heger, Woosley & Fryer 2003; Woosley & Heger 2006; Yoon, Langer & Norman 2006; Zhang, Woosley & Heger 2008; Woosley & Heger 2012). The aims of these works ranged from an investigation of the properties of GRB progenitors, to a determination of the rotational properties of the compact object remnants, to the yields of heavy elements produced by nucleosynthesis. Among the studies specifically devoted to fallback disk formation, the focus has been on the compact, hyperaccreting disks believed to power GRBs.

In this paper we take a new look at the problem of massive star collapse, by concentrating our numerical study on the properties of the fallback material that does not hyperaccrete rapidly onto the newly born compact object, but that is instead able to form a long-lasting accretion disk. We take advantage of the recent inclusion of stellar rotation in the public MESA code for stellar evolution (Paxton et al. 2013), which allows us to run a large grid of models. Our study is aimed at determining the range of initial conditions (mass, circularization radius) of the fallback material as a function of mass and angular momentum of the progenitor star, both for the BH and the NS remnant cases. For the special case of the NS remnants (not treated so far in the numerical literature), we aim at assessing whether the properties of these fallback disks around newly born NSs are consistent with those needed to explain a wide range of NS phenomena as described above.

Our paper is organized as follows: in Sec. 2 we describe the grid of main sequence star models that we use (60 models, organized in a grid of 3 metallicities, 4 masses, and 5 initial angular velocities), and how they are evolved with MESA. Given the importance of magnetic torques in the transfer of angular momentum between various layers, we further explore, for a subset of cases, the dependence of the pre-SN angular momentum on the presence (or not) of such magnetic torques. Sec. 3 describes how the stars are exploded, and the resulting fallback mass as a function of explosion energy and initial star configuration. Sec. 4 takes the results from Sec. 2 and 3 in order to evaluate the properties of the stars for which fallback disks are expected, and, when so, to compute their initial properties and estimate their time evolution. We find that extended, long-lived disks around isolated NSs require very fine-tuned initial conditions, and hence they are not expected to be a common outcome of SN explosions. Extended, long-lived disks could instead be found around BHs of $M \gtrsim 10 - 15 M_{\odot}$, with conditions possibly suited to planet formation. We summarize our findings in Sec. 5.

2. MASSIVE STAR MODELS AND THEIR PRE-SUPERNOVA ANGULAR MOMENTUM DISTRIBUTION

The fate of fallback matter after the SN explosion is primarily determined by two factors: the angular momentum distribution of the pre-SN star, and the explosion energy during the SN. The former determines whether there is *any* matter with specific angular momentum larger than the local Keplerian value, while the latter determines whether that high- j matter remains bound and hence can circularize around the newly born compact object. We describe in this section the computation of the pre-SN models, while in the following section we describe how the stars are exploded.

We compute the pre-supernova angular momentum profiles by evolving star models with the state-of-the-art open source code MESA (Paxton et al. 2011, 2013). This code includes the physics of rotation, the implementation of which has been extensively discussed in Paxton et al. (2013). We refer to this latter work for the details of the angular momentum transport mechanisms due to rotation and magnetic torques adopted in this paper.

A number of studies (Maeder 1987; Yoon & Langer 2005; Woosley & Heger 2006; Yoon et al. 2006; Paxton et al. 2013) have shown that, at a certain threshold (surface) rotation rate $(v_{\text{surf,ini}}/v_{\text{crit}})_{\text{thres}}$, the evolution on the H-R diagram bifurcates. The critical surface equatorial velocity v_{crit} is defined as

$$v_{\text{crit}}^2 = \left(1 - \frac{L}{L_{\text{Edd}}}\right) \frac{GM}{R} \quad (1)$$

where R is the radius of the star of mass M , and $L_{\text{Edd}} = 4\pi cGM/\kappa$, with κ the opacity. Above this threshold, internal mixing processes are able to inhibit the formation of a strong compositional gradient in the star, which is otherwise built by nuclear burning in the stellar core. What ensues is a chemically homogeneous evolution. Stars evolving this way avoid a core-envelope structure and become compact Wolf-Rayet stars already during H-burning. Their core, which is not dramatically spun down by coupling with an extended envelope, retains a high angular momentum prior to collapse if the wind mass-loss is not too strong (e.g. at low metallicity). On the other hand, stars below this threshold undergo a “canonical” evolution and experience a RSG phase, with their core losing a substantial amount of angular momentum. The precise value of $(v_{\text{surf,ini}}/v_{\text{crit}})_{\text{thres}}$ is firstly a function of the mass of the star, with a further dependence on metallicity. More massive stars evolve chemically homogeneously at a lower value of $(v_{\text{surf,ini}}/v_{\text{crit}})$. This is because the Eddington-Sweet circulation, which, beside convection, is believed to be the dominant mixing process during the main sequence of rotating massive stars, has a timescale proportional to the Kelvin-Helmholtz time scale, $\tau_{\text{ES}} \propto \tau_{\text{KH}} (v_{\text{surf,ini}}/v_{\text{crit}})^{-2}$. For main sequence stars the Kelvin-Helmholtz timescale decreases with increasing mass. Moreover, in massive stars the increasing radiation pressure weakens the entropy barrier, resulting in more efficient internal mixing (Yoon et al. 2006). On the other hand, higher metallicity means an increasing amount of mass loss (and hence angular momentum loss) through line-driven winds. This tends to slow the star down, requiring a larger value of $(v_{\text{surf,ini}}/v_{\text{crit}})$ for the star to follow the chemically homogeneous branch. Note that even if a star begins evolving chemically homogeneously on the zero age main sequence, its wind can quickly remove angular momentum and the star moves back to a canonical evolution. In our calculations mass loss has been implemented according to the recipe described in Yoon et al. (2006). Note that massive rotating stars can approach critical rotation during their evolution, which is expected to lead to an enhancement of the stellar mass loss. This is calculated according to the prescription (see Sec. 6.4 in Paxton et al. 2013)

$$\dot{M}(\Omega) = \dot{M}(0) \left(\frac{1}{1 - \Omega/\Omega_{\text{crit}}} \right)^{0.43}, \quad (2)$$

where Ω is the surface angular velocity, and Ω_{crit} is the critical angular velocity at the surface ($\Omega_{\text{crit}}^2 = (1 - L/L_{\text{Edd}}) GM/R^3 = v_{\text{crit}}/R_{\text{crit}}$, where R_{crit} is the equatorial radius at breakup, which is 1.5 times the polar radius).

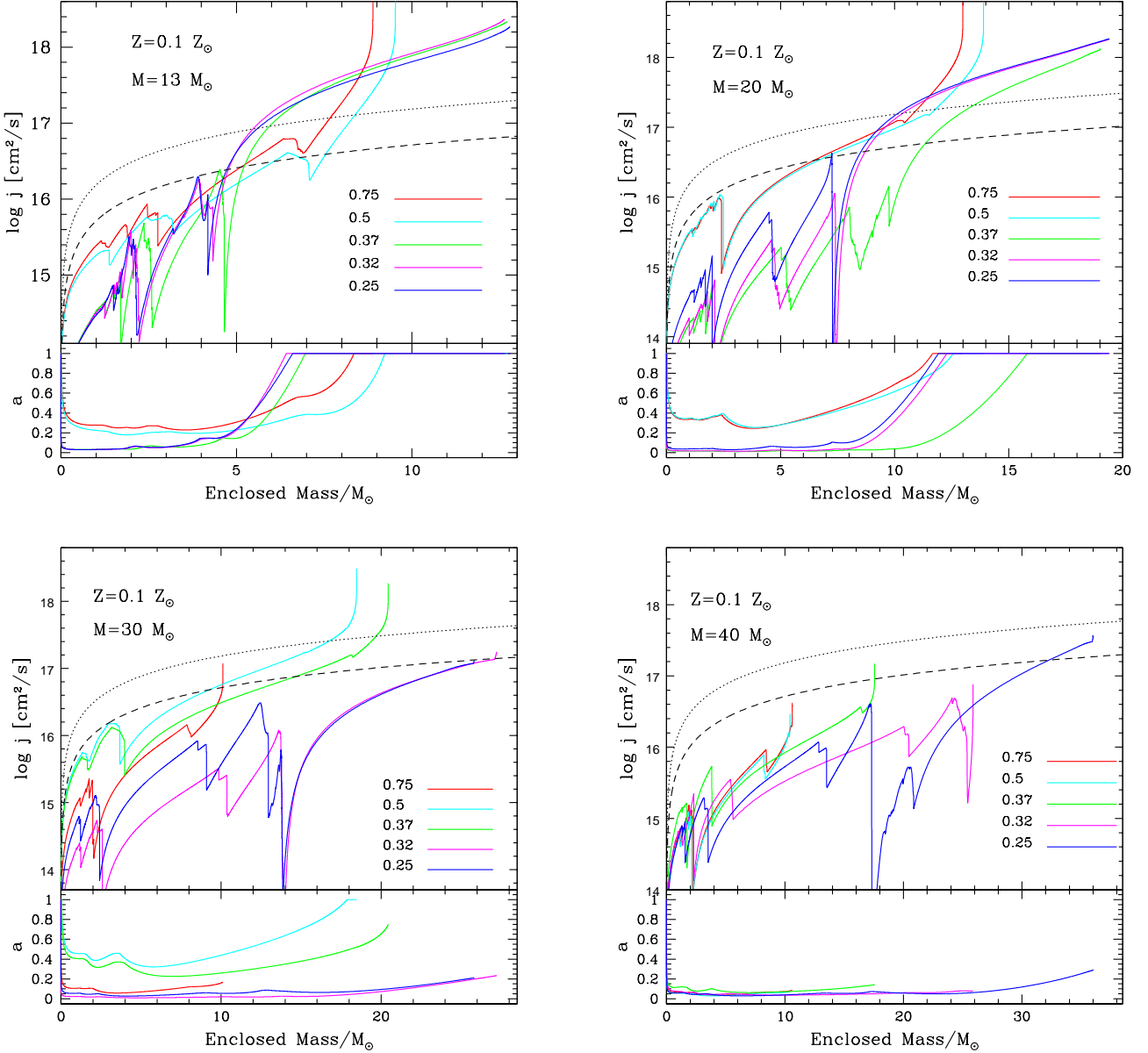


FIG. 2.— Same as in Fig 1, but for main sequence stars of 10% solar metallicity.

The mass loss timescale is limited to the thermal timescale of the star τ_{KH}

$$\dot{M} = \min \left[\dot{M}(\Omega), 0.3 \frac{M}{\tau_{\text{KH}}} \right]. \quad (3)$$

Convective regions are determined according to the Ledoux criterion. Semiconvection according to the prescription of Langer et al. (1983) is used, with a parameter $\alpha_{\text{sc}} = 1.00$.

In order to explore a significant parameter space in velocity, mass, and metallicity, we use MESA to evolve a grid of 60 models, characterized by 3 values of metallicity, ($Z = 1\%$, 10% and 100% Z_{\odot}), 4 values of mass ($M = 13, 20, 30, 40 M_{\odot}$), and 5 values of surface rotation velocity ($v_{\text{surf,ini}} = 0.25, 0.32, 0.37, 0.5, 0.75 v_{\text{crit}}$). As our “standard” set of models, we consider calculations that include internal angular momentum transport by magnetic torques. These magnetic fields arise in radiative zones and are believed to be produced by dynamo action transforming part of

the rotational energy into magnetic energy (Spruit-Tayler dynamo; Spruit 2002). While the reality of this dynamo loop in stars is currently debated (e.g., Braithwaite 2006; Zahn et al. 2007), models including this extra angular momentum transport mechanism do a much better job predicting the final spin rate of compact remnants (Heger et al. 2005; Suijs et al. 2008). Therefore, we have adopted here as our standard evolution one that includes magnetic coupling. However, for a few significant cases, we also explore the influence on the results of the lack of magnetic fields during evolution. Whenever we need to refer to a specific model within the standard set, we will use the notation $Z_{xx}M_{yy}v_{zz}$, where xx is the percentage of solar metallicity, yy is the mass in solar units, and zz is the percentage of the critical velocity.

The MESA runs are set up to proceed until the onset of core collapse, defined as the moment when any part of the Fe core is falling with a velocity $v \geq 1000 \text{ km s}^{-1}$; however, for

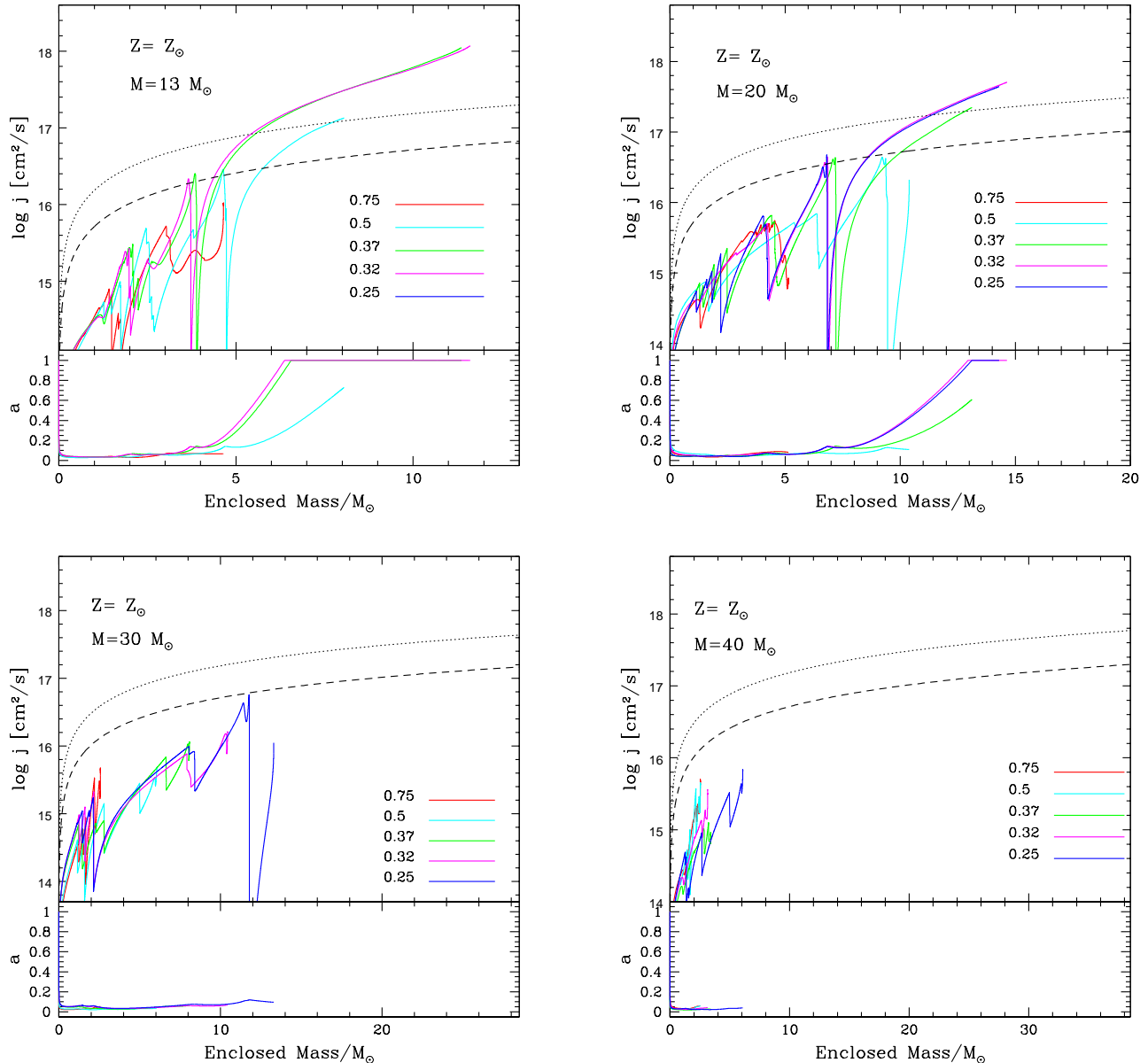


FIG. 3.— Same as in Fig 1, but for main sequence stars of solar metallicity.

some models, the timestep adopted by MESA past core Carbon burning become prohibitively small. As at this time the star has only a few years to live, the amount (and distribution) of angular momentum is not expected to change substantially. Therefore the conclusions that we draw on the angular momentum distribution of the fallback matter are expected to remain robust, regardless of the particular endpoint, past core C-burning, chosen for the model.

Models at solar metallicity have been evolved using an artificial reduction of the superadiabaticity ($\delta\nabla \equiv \nabla_T - \nabla_{\text{ad}}$) in radiation dominated convection zones. Here ∇_T and ∇_{ad} are the actual temperature gradient and the adiabatic temperature gradient, respectively. This reduction is applied in regions where the mixing length theory (MLT) is out of its domain of applicability and MESA (like other 1D stellar evolution codes) struggles with very short timesteps. This approach (MLT++) is thoroughly described in Paxton et al. (2013). In this study

we reduced the superadiabaticity of $Z = Z_\odot$ models by a factor 10^{-2} when $\delta\nabla > 10^{-4}$.

Figures 1, 2, 3 show the specific angular momentum distribution in the pre-SN stars for three values of the metallicity ($0.01Z_\odot$, $0.1Z_\odot$ and Z_\odot), and a range of ZAMS rotational velocities between 0.25 and 0.75 of the critical value. For each of the models, we also show the distribution of the spin parameter $a = J/M$ of the enclosed mass.

While the above are our “standard” model, we also consider, for a few cases, how the pre-SN angular momentum distribution is modified in the case of no magnetic coupling. Since this is of particular relevance for the possibility of forming fallback disks around NS remnants, we consider models which leave behind a NS. Figure 4 shows a comparison between models with and without B fields, for two solar metallicity models with mass 16 and 20 M_\odot and a rotational velocity of $v_{\text{surf,ini}}/v_{\text{crit}} = 0.2$ and $v_{\text{surf,ini}}/v_{\text{crit}} = 0.25$. Also indicated

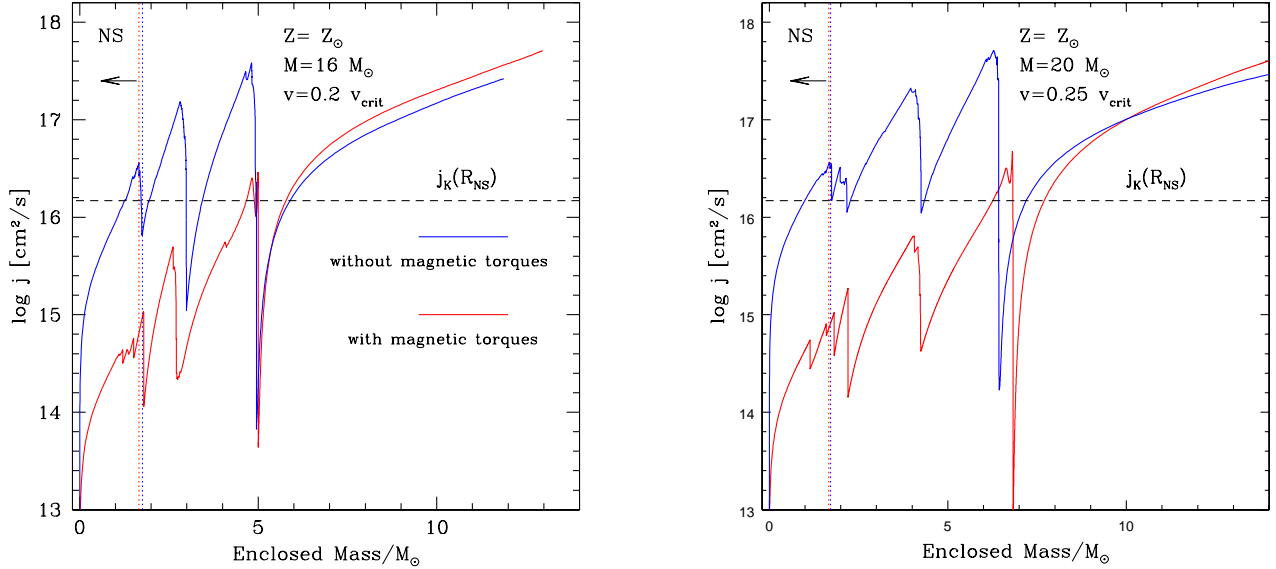


FIG. 4.— Comparison between the distributions of specific angular momentum in the pre-SN star with and without the inclusion of magnetic torques. These stars, at solar metallicity, leave behind a NS remnant. The dashed horizontal line indicates the specific angular momentum needed for circularization at the NS radius, for a typical $R = 10$ km. The region to the left of the vertical lines indicates the mass which collapses to a NS.

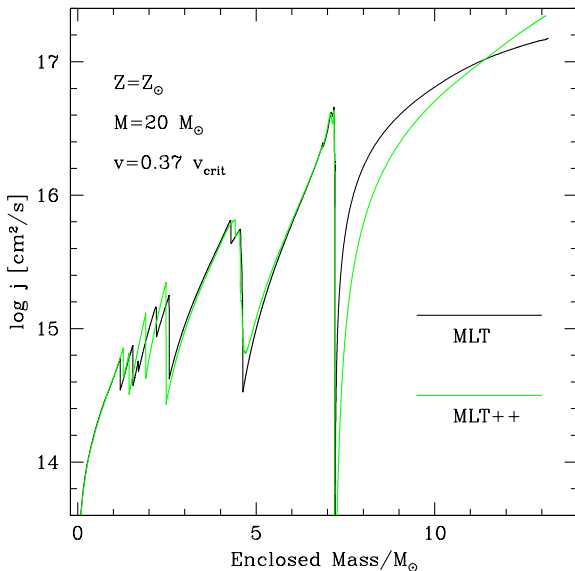


FIG. 5.— Comparison between the distributions of specific angular momentum in the pre-SN star with and without the reduction of superadiabaticity in radiation dominated envelopes (MLT++). The comparison is for a $20M_{\odot}$ model at $Z = Z_{\odot}$ initially rotating at 37% of critical velocity.

is the minimum specific angular momentum for material to circularize just outside of a NS of mass equal to that of the iron core in the simulation, and a typical radius of 10 km. It is evident how the lack of magnetic torques results in a substantially larger specific angular momentum in the layers outside of the iron core. This is because the core of the star evolves essentially decoupled from the envelope, and is able to retain a large fraction of its initial angular momentum.

To assess the effect of the adoption of the MLT++ in our solar metallicity models, we evolved a $20M_{\odot}$ model initially rotating at 37% of its critical velocity, with and without the reduction of the superadiabaticity. A comparison of the final angular momentum distributions is shown in Fig. 5, revealing

minimal differences between the two calculations. For models above $\sim 25M_{\odot}$ at solar metallicity, similar tests cannot be performed, as in that case calculations that do not include the MLT++ cannot reach core collapse (this is the reason why MLT++ has been implemented in the first place, see Paxton et al. 2013). In general, we expect the integrated mass and angular momentum loss to be affected by the adoption of MLT++, since this tends to change the surface stellar radius (hence surface temperature, entering the calculations of the mass loss rate). Such uncertainty is even larger for rapidly rotating models, where the evolution of the stellar radius (affected by the efficiency of energy transport in the stellar envelope) has an important role in determining the amount of mass lost at critical rotation. Until a better theory for energy transport in radiation dominated zones is available, we have to consider these results highly uncertain. Since the models at solar metallicity have not been considered for the explosion calculations (disk formation is marginal for $Z = Z_{\odot}$), the adoption of MLT++ does not affect the stellar explosions calculations presented in Sec. 3 and, overall, the major conclusions of this paper.

The fate of the material ejected during the explosion depends on both its specific angular momentum, as well as on the energy of the explosion, which determines the amount of mass that remains bound, and hence falls back. The latter is discussed in the following section.

3. STELLAR EXPLOSIONS AND THEIR FALLBACK MASS

The fallback dynamics are computed by means of direct numerical calculations of the explosion. These calculations are performed using a one-dimensional version of the TESS code (Duffell & MacFadyen 2011, 2013). TESS is a multi-dimensional moving-mesh hydrodynamics method, which is both Lagrangian and shock-capturing. As a result, the expansion of the shock through the many layers of the star is captured very accurately.

Each calculation is initiated as follows: The final state of a MESA run is used as initial conditions for the density and pressure of the star. The mass of the iron core is subtracted from this density profile and re-introduced as a point mass, to

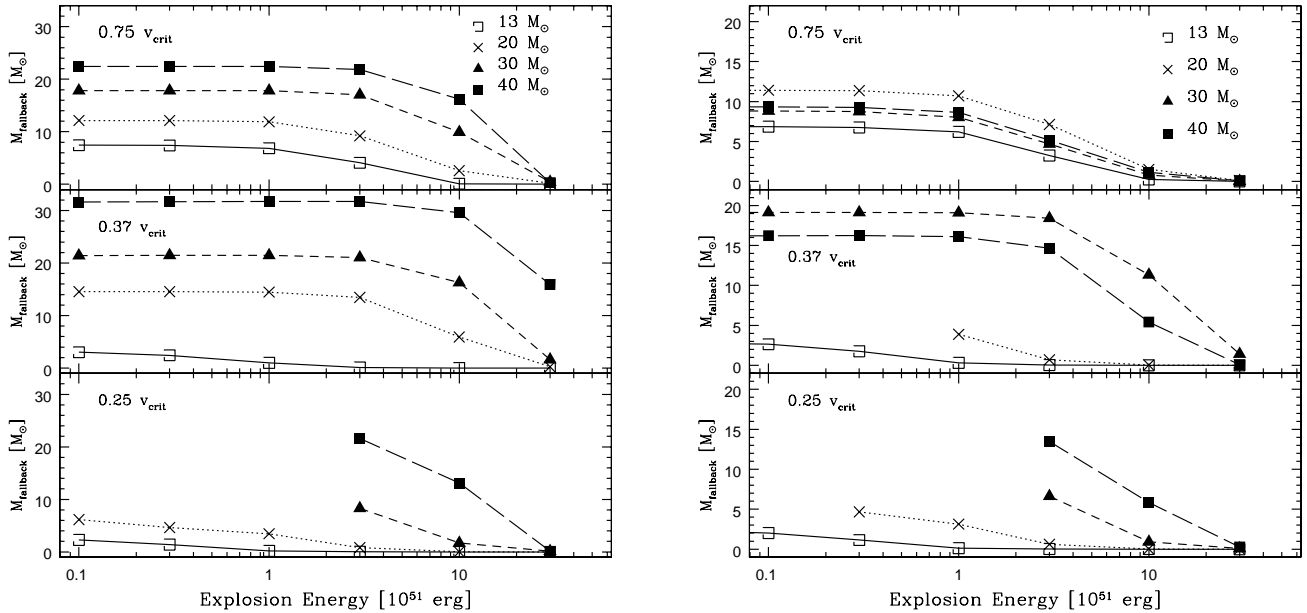


FIG. 6.— Fallback matter (i.e. amount of mass which remains bound) as a function of the explosion energy for stars with metallicity $Z = 0.01Z_{\odot}$ (left panel) and $Z = 0.1Z_{\odot}$ (right panel), and for the ‘standard model’ with magnetic torques. Results for three values of the initial rotational velocity of the star are displayed. We have not displayed the data points for those simulations for which the shock had not had yet the time to cross the outer layers of the star during the run time of the simulation. This is the case for those stars which do not undergo significant mass loss during their evolution, and hence have extended envelopes in the pre-SN state.

simulate the formation of the compact object. A fixed thermal energy is then added within a small radius (1.5 times the radius of the core), which causes an expansion and accelerates a shockwave which pushes its way out of the star. The inner boundary is initially reflecting for the first phase of evolution, as the gas is accelerating. After this thermal energy has been converted into kinetic energy in the shockwave, fallback can begin (this typically takes about 10 seconds). At this point, we switch the boundary to be absorbing, and mass can freely pass through the inner boundary and be added to the compact point mass at the origin. After the shock has crossed a given radius r , fluid elements interior to this radius have been accelerated and can either escape the gravitational potential of the interior mass, or freely fall back. At any given time, we can define a critical radius, r_{bound} , as the largest radius such that all material interior to it is bound. We calculate this radius and measure the amount of mass in its interior, $M_{\text{bound}}(t)$, as a function of time. At late times, this mass asymptotes to a finite value $M_{\text{bound}}(\infty) \equiv M_{\text{fallback}}$, which is the total fallback mass.

For each pre-SN model, we simulated the star explosion for a broad range of explosion energies. We note that the mechanism for core collapse supernova explosions remains a topic of current intensive research. Indeed, many detailed numerical simulations (e.g. Herant et al. 1994; Burrows et al 1995; Woosley & Janka 2005; review by Janka et al. 2007 and references therein) are not able to achieve a successful explosion, especially for the higher mass stars. Since the explosion dynamics depends on complex non-linear interactions between neutrinos interacting with fluid in a turbulent ‘‘gain’’ region (e.g. Liebendorfer et al. 2005), it is still not possible at present to calculate the explosion energy with any certainty. In the future, high resolution 3D simulations with full neutrino transport schemes may be able to solve this problem. Lacking a definitive detailed calculation for the explosion dynamics, the

precise kinetic energy released must be constrained by observations. Here we have used a range of kinetic energies consistent with observations as well as with the recent literature (e.g. Nomoto et al. 2006; Mazzali et al. 2013).

Fallback masses for a range of star models and explosion energies are plotted in Figure 6; in particular, for the standard models with magnetic coupling, we simulated the explosion of stars with metallicities of 1% and 10% of the solar value, since the possible formation of a disk is marginal at solar metallicity in these models.

Note that, due to computational limitations, we do not explicitly evolve the system to all the way to fallback, as this process can take an arbitrarily large amount of time for marginally bound fluid elements. Typically we evolve the system for a time $t_{\text{fin}} = 2 \times 10^3$ seconds. We should further note that, for some models, this running time is not even enough for the shock to push its way through the entire star. In particular, models with extended envelopes which have not undergone substantial mass loss take a very long time for the shock to cross the star ($\sim 10^7$ seconds). This was generally found to be the case in the models with slow rotation ($v_{\text{surf,ini}} = 0.25v_{\text{crit}}$), and also for the 10% metallicity example at moderate rotation ($v_{\text{surf,ini}} = 0.37v_{\text{crit}}$). Longer run-times are computationally expensive, especially given the large number of models and explosion energies being calculated here. However, for these cases, the outer layers of gas have a relatively low binding energy, and hence even a very weak explosion can unbind this mass. If the explosion energy is much larger than this binding energy, we expect the results to not depend sensitively on the outer layers. For a few of the models (in particular Z1M13v32 and Z10M13v32, see Sec. 4.2.2), we have explicitly run the calculation to a much longer time, $t_{\text{fin}} = 10^7$ seconds, to verify that these outer layers do indeed behave as we expect them to.

For the reasons mentioned above, we have found in practice that the details of these marginally-bound outer layers are

only important for very weak explosions. For these models, we have omitted the low-energy results from Figure 6, so that the only data included represent simulations for which either the shock has crossed the star, or the outer layers do not significantly affect explosions of the given energy.

4. POST-SN DISK FORMATION, EVOLUTION, AND OBSERVABILITY

In the following, we couple the results from the previous two sections to discuss the post-SN phenomenology of the ejected material. We treat the NS and BH cases separately.

For each star model, in order to establish whether the iron core immediately collapses to a NS or a BH, we track its mass. For the models we studied, masses are below $\sim 2.1M_\odot$ in all the cases. A NS is expected to be the common outcome of the implosion of the iron core immediately after the SN explosion¹. However, for a large range of explosion energies enough material is expected to fall back and form a BH. BH formation from fallback has been widely discussed in the literature (e.g. Heger et al. 2003). In the following, for both NSs and BHs, we will focus our discussion on the angular momentum of the material that falls back, and hence on the possibility of the existence of a short or long-lived fallback disk.

For a fallback disk to be formed, a fraction of material must remain bound, and it must possess a specific angular momentum j_m at least as large as the angular momentum at the last stable orbit, j_{ls} .

The bound fraction of the stellar envelope at radius R will fall back on a timescale on the order of the free-fall time

$$t_{ff}(r) = \pi \sqrt{\frac{R^3}{8GM}}, \quad (4)$$

where M is the enclosed mass inside radius r . The maximum radial distance, r_{\max} , reached by each parcel of material is determined by the details of the explosion, with the explosion energy playing the most important role. We compute the post-explosion density profile of the gas as described in Sec. 3.

Each bound parcel of gas, of specific angular momentum j_m , after falling back will circularize at a radius R_{circ} given by the solution of the equation $j(R_{\text{circ}}) = j_m$. Once the bound material has fully circularized in a ring, the following evolution occurs on the viscous timescale²

$$t_0(R_{\text{circ}}) = \frac{R_{\text{circ}}^2}{H^2 \alpha \Omega_K} \sim 275 \alpha_{-1}^{-1} m_{10}^{-1/2} R_{10}^{3/2} \left(\frac{R}{H}\right)^2 \text{ s}, \quad (5)$$

where $m_{10} = M/(10M_\odot)$, $R_{10} = R/(10^{10} \text{ cm})$, Ω_K is the Keplerian velocity of the gas in the disk, H the disk scale-height, and α the viscosity parameter (Shakura & Sunyaev 1973), written in units of $\alpha_{-1} \equiv \alpha/0.1$.

The accretion rate at early times, while fallback still proceeds, is determined by the longer of the two timescales above. The subsequent evolution of the material, and its observable phenomenology, will depend on the initial \dot{M} , as well as on the location at which the fallback ring of material circularizes.

In the following, we will discuss the expected initial conditions of the high- j fallback material for the wide range of progenitor stars and explosion energies considered here.

¹ These results are consistent with the findings of Heger et al. (2003). They found that only for initial star masses $M \gtrsim 40M_\odot$ (and sub-solar metallicity) a BH can be formed by direct collapse.

² We note that, while Eq. (5) represents the classical viscous timescale, material can flow at a faster rate if transition fronts (see e.g. Menou et al 1999) are present (Cannizzo 1998; Kotko & Lasota 2012).

4.1. Fallback and disk formation around Neutron Stars

We begin with the discussion of the expectations for our standard models with magnetic torque. The remnant compact objects are NSs for strong explosions, with the precise value of E depending on M, Z, v .

Inspection of Figs. 1, 2 and 3 shows that, if the stellar evolution proceeds under conditions of strong magnetic coupling, the outermost shells of material surrounding the newly born NS *never* possess sufficient angular momentum to be able to circularize into a disk, even for the fastest rotating main sequence stars at low metallicity. The circularization radius for the small shells of material just outside the NS is at most a couple of kilometers for the most favorable scenarios. In these situations, if those shells are not ejected during the explosion, that material will fall back and impinge on the NS surface before completing a full orbit. These sudden episodes of accretion might give rise to X-ray flashes immediately following the NS birth. However, the high opacity of the stellar envelope at those early times (e.g. Chevalier & Fransson 1994) will make these re-brightenings difficult to observe.

The fate of the fallback material after the SN explosion is expected to be very different if magnetic torques do not play any significant role during stellar evolution. To explore this scenario, we ran two new sets of models; each set has the same Z, M, v , but one case is with magnetic torques, and the other without. The comparative results are displayed in Fig. 4, for stars of solar metallicity. It is apparent that, lacking magnetic torques to slow down the interior layers, there is plenty of material with specific angular momentum large enough to circularize outside of the NS radius. However, the explosion energy needs to be rather fine-tuned so that not all the outer layers are ejected, nor too much of them falls back causing prompt collapse to a BH.

Let's consider the case that the explosion energy happens to be just about right so that only a small fraction, say $\lesssim 0.1M_\odot$, falls back. With the initial collapsing core $\sim 1.7M_\odot$ in the considered model, such a fallback mass amount ensures that the compact remnant remains an NS. We exploded the Z100M16v20 model shown in Fig. 4 (left panel, profile without magnetic torques) and found that, for an explosion energy $\sim 3 \times 10^{52}$ erg, about $0.08M_\odot$ of solar mass remains bound, while the rest of the envelope gets unbound. This bound $\sim 0.08M_\odot$ is located at a radius of about 2.6×10^8 cm in the pre-SN star. Our fallback calculations find that the outermost radial distance that this bound shell of material reaches during the explosion before turning back is $r_{\max} \sim 1.8 \times 10^{10}$ cm. The free-fall time of this material is on the order of a few hundred seconds, and its circularization radius is at about 1.7×10^6 cm.

The time-dependent fallback accretion rate of the bound $0.08M_\odot$ shell of material is displayed in Fig. 7. The temporal power-law decay, $\sim t^{-5/3}$, has been found before in similar types of fallback calculations (MacFadyen et al 2001), which relied on an alike density profile to ours.³ Since

³ The semi-analytical fallback calculations of Kumar et al. (2008) also found an initial rate of fallback $\propto t^{-5/3}$, followed by a steeper decay after a few hundreds of seconds, which, in their particular progenitor model, corresponded to a drop in the density profile. A direct correspondence between the fallback timescale in their model and ours (as well as that of MacFadyen et al. 2001) cannot be made, since their computation did not include a simulation of the explosion and the consequent fallback delay due to the shock pushing out the material before it starts to fall back. Also, if the explosion is strong and most of the material gets unbound such as in the case of Fig. 7, then the steepening in \dot{M} is not seen since the outer parts of the star envelope, where the density drops, have become unbound.

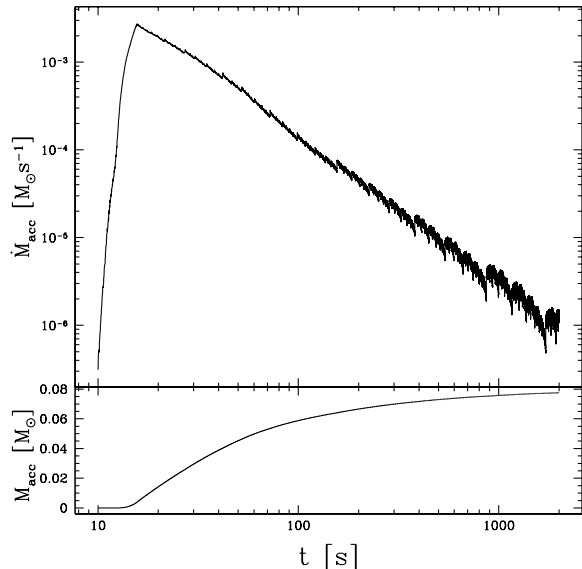


FIG. 7.— Accretion rate (*top panel*) and total accreted mass (*bottom panel*) for the Z1M16v20 model with no magnetic torques, and an explosion energy of 3×10^{52} erg. For this explosion energy, only $\sim 0.08 M_{\odot}$ remains bound and falls back, and the remnant compact object remains an NS.

the viscous timescale t_0 at the circularization radius is very short (about a millisecond), and hence $t_0 \ll t_{ff}$, the disk can be imagined as evolving through a series of steady-state configurations at very high accretion rates, varying between $\sim 10^{-3} M_{\odot} \text{ s}^{-1} - 10^{-6} M_{\odot} \text{ s}^{-1}$ within a few hundred seconds. This is an accretion regime known as hyperaccretion.

Hyperaccretion around an NS, unlike the BH case, has received a rather limited attention in the literature. Kohri et al (2005) analyzed the problem with the aim of searching for an extra energy source which may help supernova explode in numerical simulations. They pointed out how, due to the very high accretion rates, the accretion flow, once circularized into a disk, would be a neutrino-dominated accretion flow (NDAF; Popham et al. 1999; Narayan et al. 2001; Kohri & Mineshige 2002). Their analysis showed that, under a wide range of conditions, strong outflows would develop, and carry away a large fraction of mechanical energy. This energy might then help in producing a successful supernova explosion.

More recently, Zhang & Dai (2008, 2009) studied the structure of a steady-state hyperaccretion disk around an NS, motivated by suggestions that the collapse of a massive star giving rise to a GRB might be powered by accretion onto an NS instead of a BH. A fundamental difference between hyperaccretion onto an NS and onto a BH derives from the fact that the BH has an event horizon, while the NS has a hard surface. As a result, if the accreting object is a BH, the internal energy in the accretion flow can be advected inward into the event horizon without any energy release. On the other hand, if the accreting object is an NS, the internal energy must eventually be expelled from the disk, since the NS surface prevents energy advection into the star. A hyperaccreting disk around an NS, similarly to the BH case, is very hot and dense, optically thick to photons, and hence cooling is dominated by neutrinos. The presence of the boundary layer at the NS surface, and the consequent inability of the NS to advect energy, causes an higher neutrino luminosity than in the case of BH hyperaccretion. Such explosive events could therefore power long GRBs. However, a quantitative comparison between the

fallback accretion rate predicted by our numerical simulations (cfr. Fig.7), and the temporal evolution of the luminosity observed in long GRBs (e.g. Zhang et al. 2006) cannot be reliably made at this stage. As discussed above, the detailed way by which hyperaccretion around an NS proceeds is not well known. Furthermore, the efficiency by which the fallback accretion rate gets converted into accretion rate onto the NS and/or into winds must be changing with time, depending on the magnitude of the fallback rate itself, since the accretion mode depends on \dot{M} , and the accretion rate onto the NS surface must remain Eddington limited. And this is in addition to the uncertainty with which the accretion energy is then converted into γ -rays during the prompt phase. Also note that, if the remnant compact object is a rapidly spinning, highly magnetized NS as suggested as an alternative model for the long GRB engine (Metzger et al. 2011), then the energy output (and hence the possible signatures in the light curves) may be dominated by the electromagnetic component rather than the accretion one.

The above studies highlight the importance of the formation of hyperaccreting disks around NSs for supernovae and Gamma-Ray Bursts. Our investigation shows that such disks can be formed, but under special conditions: (i) magnetic breaking must not be effective during the progenitor star evolution; (ii) the explosion energy must be fine-tuned so that a fraction of mass remains bound, but only a small fraction, not exceeding a few tens of solar mass in order for the NS to remain stable, or else it would produce an accretion induced collapse of the NS into a BH, also characterized by an early hyperaccreting phase (Giacomazzo & Perna 2012).

The disks discussed above, independently of their specific structure, and the presence or not of outflows, are characterized by being highly transient, with relatively short durations of at most several hundreds of seconds. Given their formation within a few Schwarzschild's radii, these disks get rapidly depleted before they can expand to sufficiently large radii and form the extended, low-accretion, and long-lived disks ($10^4 - 10^5$ yr) which have been widely discussed in the NS literature, as summarized in the introduction. Therefore, we can robustly conclude that *long-lived fallback disks around isolated NSs are not expected to be common*. Their formation would require a set of very fine tuned conditions, such as an explosion which is strong enough to unbind the innermost layers surrounding the NS, but anisotropic in such a way that some of the outer, high- j layers were not affected and could fallback on a much longer timescale at much larger radii. Mixing between layers with different initial angular momentum could further occur due to hydrodynamic instabilities (e.g. Fryxell, Arnett & Mueller 1991; Chevalier, Blondin & Emmering 1992). However, whether these instabilities could possibly lead to the formation of a small-mass disk at larger radii (with everything inside emptied to avoid the accretion induced collapse of the NS to a BH) would have to be investigated through detailed numerical simulations.

The above considerations have not considered the potentially important effect of the interaction between the accreting matter and strong magnetic fields in the newly born NSs. This is a topic which has received a considerable degree of attention in the literature, both analytically and semi-analytically (e.g. Illarionov & Sunyaev 1975; Ghosh & Lamb 1979; Lovelace et al. 1995, 1999; Ikhshanov 2002; Rappaport et al. 2004; Eksi et al. 2005; D'Angelo & Spruit 2010; Piro & Ott 2011), as well as numerically (e.g. Hayashi et al. 1996; Miller & Stone 1997; Fendt & Elstner 2000; Matt et al. 2002; Ro-

manova et al. 2004, 2009). A strong magnetic field exerts a pressure on the accretion flow, which is able to balance the ram pressure of the accreting material at a radius on the order of the magnetospheric radius, $R_m = [\mu^2/(2GM)^{1/2}\dot{M}]^{2/7}$, where μ is the magnetic stellar moment (e.g. Davidson & Ostriker 1973). This radius defines approximately the inner boundary of the accretion disk. A magnetized NS is able to accrete only under the condition that, at the magnetospheric radius, the velocity of the rotating magnetosphere (equal to the stellar angular velocity Ω_0) is smaller than the local Keplerian velocity of the disk material, $\Omega_K(R_m)$; if this condition is not satisfied, a centrifugal barrier will inhibit accretion (Illarionov & Sunyaev 1975). The above condition can be equally reformulated by stating that the magnetospheric radius must be smaller than the corotation radius $R_{co} = (GM/\Omega^2)^{1/3}$, which is the radius at which the Keplerian frequency of the orbiting matter is equal to the NS spin frequency. For a hypothetical fallback disk not to be influenced by the magnetic field of the NS, the magnetospheric radius must not be larger than the corotation radius, which yields a lower limit onto the accretion rate,

$$\dot{M} > \dot{M}_{\text{prop,crit}} = 6 \times 10^{-9} \mu_{30}^2 M_{1.4}^{-5/3} P_1^{-7/3} M_\odot \text{ s}^{-1}, \quad (6)$$

where $\mu_{30} \equiv \mu/10^{30} \text{ G cm}^3$, $P_1 \equiv P/1 \text{ s}$, $M_{1.4} \equiv M/1.4M_\odot$. Other effects (related to the presence of magnetic fields) which can hinder the formation of a disk are dipole spin-down radiation and a neutrino-driven, magnetically-dominated wind (Thompson et al. 2004; Piro & Ott 2011). These yield, respectively, further limits on the accretion rate,

$$\dot{M} > \dot{M}_{\text{dip,crit}} = 1.8 \times 10^{-11} \mu_{30}^2 M_{1.4}^{-1/2} P_1^{-4} R_{12}^{1/2} M_\odot \text{ s}^{-1}, \quad (7)$$

and

$$\dot{M} > \dot{M}_{\nu,\text{crit}} = 5.4 \times 10^{-8} \mu_{30}^{4/5} M_{1.4}^{-1/2} P_1^{-8/5} \dot{M}_{\nu,-3}^{3/5} R_{12}^{1/2} M_\odot \text{ s}^{-1}. \quad (8)$$

In the above equations, $R_{12} \equiv R/12 \text{ km}$, and $\dot{M}_{\nu,-3} \equiv \dot{M}_\nu/10^{-3} M_\odot \text{ s}^{-1}$ is the mass-loss rate caused by the neutrino-driven wind.

In the case of the disks produced under the conditions discussed above (negligible magnetic torques, strong explosion that leaves only the innermost few tens of solar masses bound), we find that the very high accretion rates, $\dot{M} \gtrsim 10^{-6} M_\odot/\text{s}$, generally dominate over magnetic effects unless the NS is born with a magnetar-type field, and with a period on the order of the millisecond. In these cases, the NS-disk system would be in the propeller phase, and the disk may be disrupted through a combination of the transfer of accretion power and rotational power of the NS to the disk (Eksi et al. 2005).

All together, the presence of strong magnetic fields in the newly born NS would only make the formation and survival of a hypothetical fallback disk even more difficult. However, we note that a possible avenue that might create the conditions for an extended disk at larger radii could occur through 'recycling' of the matter expelled during the propeller phase, i.e. if some of the material which has gained angular momentum through momentum transfer at the magnetospheric radius during the propeller phase does not get unbound, and falls back at radii much larger than R_m (Perna, Bozzo & Stella 2006). While this is a possibility, we however note that it requires even more special conditions to be realized: negligible magnetic torques so that the innermost layers of material have $j > j_K(R)$, a strong explosion so that only a few tens of mass fall back; strong NS B field and short birth period to allow the

propeller phase to set in, anisotropic conditions in the pulsar wind outflow so that the disk is not blown away, and constraints on the parameters B , P and \dot{M} so that a fraction of the propelled material does not get unbound.

4.2. Fallback and disk formation around Black Holes

For those stars which leave behind a BH remnant, the formation of a fallback disk, while being common in the less physically relevant $B = 0$ case, is also relatively common when magnetic torques play a significant role in the post main-sequence evolution, unlike the NS remnant case. The detailed outcome is however a function of mass, metallicity and rotational speed of the main sequence star, as well as the explosion energy. For a fallback disk to be formed, a fraction of material must remain bound, and it must possess a specific angular momentum j_m at least as large as

$$j(R) = \frac{\sqrt{GMR} \left[R^2 - 2(a/c) \sqrt{GMR/c^2} + (a/c)^2 \right]}{R \left[R^2 - 3GMR/c^2 + 2(a/c) \sqrt{GMR/c^2} \right]^{1/2}}. \quad (9)$$

at the last stable orbit, where j represents the specific angular momentum of a particle on a corotating orbit of a black hole of mass M and angular momentum $J = aM$.

From the results of the grid of simulations that we have run, we distinguish two main scenarios for the ensuing observable phenomenology:

4.2.1. Hyperaccreting disks from fast-rotating/chemically homogeneous evolved stars

In our grid, for metallicities $\lesssim 10\%$ of solar, there is, for each mass value considered, a critical rotational velocity above which the evolution proceeds in a chemically homogeneous way (see discussion in Section 2). In the pre-SN phase, the star is compact and the core is fast rotating. For explosion energies $\lesssim 10^{52}$ ergs, we have found that there is always a non-negligible amount of fallback mass. The range of rotational velocities for which this fallback material is able to circularize outside the last stable orbit is an increasing function of the main sequence star mass, as discussed in Sec. 2. The free fall time of the outermost layers is typically on the order of tens of seconds, giving rise to a phase of rapid and intense accretion. These types of post-SN outcomes from massive, rapidly rotating, low-metallicity stars are believed to be the ones powering the typical long GRBs, and their properties have been widely discussed in the literature, both in the context of their formation within the SN collapse (Woosley 1993, MacFadyen & Woosley 1999; MacFadyen, Woosley & Heger 2001), as well as in the context of the post-explosion evolution, when a hyperaccreting, neutrino-cooled disk is believed to be formed (Popham et al 1999; Narayan et al. 2001; Di Matteo et al. 2002; Janiuk et al 2004, 2007; Lee & Ramirez-Ruiz 2006; Surman et al. 2006; Shibata et al. 2007; Chen & Beloborodov 2007). The duration of these disks, while varying depending on the specific angular momentum distribution of the progenitor star (e.g. Janiuk & Proga 2008), remains within at most several hundreds of seconds.

Given the extensive investigations in the literature on the topic of hyperaccreting disks around BHs and their relevance to GRBs, we will not discuss these disks any further here, and refer the reader to the appropriate literature cited above for details.

4.2.2. Long-lived disks from slow-rotating/chemically inhomogeneous evolved stars

As discussed in Section 2, for each couple of Z, M values, there exists a critical rotational velocity below which the evolution does not lead to full mixing. These stars lose substantially less mass, and hence they have a much larger radial extent in the pre-SN phase. The free fall times of the outermost layers can reach the \sim year timescale for very low-metallicity, massive stars (see also Paxton et al. 2013). By inspection of the angular momentum distribution of the chemically inhomogeneous evolved stars in Figs. 1, 2 and 3, we note that, depending on the explosion energy, there is a very large range of timescales for the bound material to fall back, all the way from milliseconds to years. Therefore, transients with durations of several days such as those observed in the sample of very long GRBs (Levan et al. 2013) should not be as surprising in the context of massive star explosions (as long as the jet still manages to penetrate the envelope). Here, we will not dwell on these intermediate-duration cases (see Woosley & Heger 2012 for a more in-depth discussion of these situations), but we will rather focus on the fate of the outermost layers of the envelope in those scenarios (weak and/or anisotropic explosion) in which these outermost layers still remain bound after the explosion, and eventually fall back.

Whether this material is able to circularize into a disk is, once again, a function of metallicity, mass, and initial rotational velocity of the MS star. For the 1% and 10% metallicity cases, the 13 and 20 M_{\odot} models display a significant range of rotational velocities for which the specific angular momentum of the fallback material is well above the required value to circularize beyond the last stable orbit. The velocity range for circularization is reduced for the higher mass models that we studied (30 and 40 M_{\odot}). However, even at solar metallicities, the two lower mass cases still display a range of rotational velocities for which the specific angular momentum of the outer envelope exceeds the circularization value at the last stable orbit.

The fate of these high- j outer layers is heavily dependent on the explosion energy. Not surprisingly, they are blown away for a wide range of explosion energies. However, for very weak explosions, the outer envelope may still remain loosely bound, and hence able to form a disk upon return. Our fallback calculations (see Section 3) which, for the Z1M13v32 and Z10M13v32 models were run for much longer timescales ($t_{\text{fin}} = 10^7$ s) and for weaker explosion energies than displayed in Fig. 6 (down to $E = 10^{48}$ erg), have shown that, for explosion energies \lesssim a few $\times 10^{48}$ erg (Z10M13v32 case) and $\lesssim 10^{49}$ erg (Z1M13v32 case), the outer layers remain bound. These scenarios lead to BHs in the $\sim 10M_{\odot}$ range, surrounded by extended fallback disks of several solar masses.

We remark that the values of the explosion energy that we quote here and throughout the text represent the isotropic values. However, if the explosion is anisotropic, as suggested by observations of SN 1987A (e.g. Hillebrandt & Höflich 1989; McCray 1993) and a number of other SNe (e.g. Fassia et al. 1998; Spyromilio 1991; Woosley et al. 1994), and a higher fraction of energy is deposited along the rotation axis, then, even an apparently rather energetic explosion could result in a relatively low amount of energy transferred to the equatorial regions, and hence a larger amount of fallback material would be available to form a disk. Alternatively, other avenues to produce fallback of the outer layers could involve very weak or absent shocks. Woosley & Heger (2012) ex-

plored this avenue in the context of blue supergiants with low mass-loss rates, tidally interacting binaries with either helium stars or giant stars, and the collapse to a BH of very massive pair-instability supernovae.

In the following, we will study in more detail the expected properties of these fallback disks, and their relevance to observations for a couple of specific cases, in particular models Z1M20v25 and Z10M13v32. We begin by estimating the initial radial extent of the disk by computing the circularization radius R_{circ} for the outermost shells, if they all fall back. In the Z1M13v37 model, the innermost $\sim 5 - 6M_{\odot}$ of material accretes rapidly onto the BH without being able to circularize. Outside of those envelope layers, the infalling material possess sufficient angular momentum to form a disk. By solving the equation $j(R_{\text{circ}}) = j_m$ as discussed above, we find that the outermost $\sim M_{\odot}$ of material circularizes in a ring between $\sim 1.4 \times 10^9 - 3.8 \times 10^9$ cm for model Z10M13v32, and between $\sim 2.7 \times 10^9 - 1.6 \times 10^{10}$ cm for model Z1M20v25. For a BH of $\sim 10 - 11 M_{\odot}$ in the former case, and of $\sim 17 - 18 M_{\odot}$ in the latter, these outermost regions correspond to ~ 1000 Schwarzschild's radii scale.

In the post explosion phase, the fallback material is very hot, and $H \sim R$, yielding $t_0 \sim 200$ s. The free-fall time is considerably longer. Even in the case of a negligible shock, i.e. with the outer layers falling back from their original location within the progenitor star, $t_{\text{ff}} \gtrsim 10^6$ s. Since $t_{\text{ff}} \gg t_0$, the initial accretion rates are on the order of $\dot{M}_d \sim \dot{M}_d / t_{\text{ff}} \sim 10^{-6} M_{\odot} \text{ s}^{-1}$. After the envelope has fully fallen back, the evolution will be driven by viscous evolution. The early times during which the accretion rate is highly super Eddington are characterized by a hot, optically thick flow, similar to the transient GRB phase, but with some important differences, and in particular, that the disk is no longer neutrino-cooled. Chen & Beloborodov (2007; see also Popham et al. 1999) find that, below a certain critical accretion rate M_c , neutrinos are no longer dominating cooling. M_c is a function of both the BH spin parameter as well as the viscosity parameter α . For $\alpha = 0.01$, neutrino cooling is negligible within $\sim 100 R_g$ for any value of the spin parameter if $M_c \lesssim 0.01 M_{\odot}$, and M_c increases with α . At the much lower fallback accretion rates expected from the outer layers of the stars under consideration, neutrino cooling will hence be unimportant. Under these conditions, accretion becomes relatively inefficient, and may proceed as an advection-dominated accretion flow (Narayan & Yi 1994, 1995). These types of flows, characterized by a positive Bernoulli constant, lose considerable mass into a wind, resulting in an accretion rate which decreases with radius. The available kinetic luminosity, on the order of $10^{46-47} \text{ erg s}^{-1}$, may however still be sufficient to power a jet, albeit much weaker than in the standard GRBs, and yield an event which, at early times, may resemble a weak and very long γ -ray transient (Quataert & Kasen 2012, Woosley & Heger 2012).

The time-dependent, long-term evolution of a hyperaccreting disk around a BH has been discussed by Cannizzo & Gehrels (2009; see also Kumar et al. 2008; Metzger et al. 2008; Cannizzo et al. 2011) in the framework of the self-similar solutions derived by Pringle (1974, 1991) for the time evolution of disks with a free outer boundary for the viscosity parameterization (without outflows). Setting the precise initial condition for the beginning of the self-similar evolution (post-fallback phase) is not a trivial issue. During the long fallback period, the very short viscous timescale causes previous rings of fallback material to quickly spread; the inner

layers accrete onto the BH, while the outer edge moves to increasingly outer radii. Fresh material that falls back may then interact and shock with the older circularized material rings. In the following, we will focus on the fate of the outermost, highest j layers of the envelope, which fall back last and circularize at radii in the range of a few $\times 10^9$ - a few $\times 10^{10}$ cm. In the super-Eddington slim disk model, and for timescales longer than the viscous time t_0 , the time evolution of the disk mass M_d , of its accretion rate \dot{M}_d , and of its radius R_d can be approximated by the self-similar solutions

$$M_d(t) = M_d(t_0) \left(\frac{t}{t_0} \right)^{-1/3}, \quad (10)$$

$$\dot{M}_d(t) = \dot{M}_d(t_0) \left(\frac{t}{t_0} \right)^{-4/3} \quad (11)$$

$$R_d(t) = R_d(t_0) \left(\frac{t}{t_0} \right)^{2/3}, \quad (12)$$

under the assumption of negligible mass outflows (and hence radius-independent mass accretion rate; Kumar et al. 2008; Metzger et al. 2008; Cannizzo et al. 2011). At this rate of accretion, the flow becomes sub-Eddington after about 10 years (scaling in units of a BH mass of $15 M_\odot$ and a ring initially at 10^{10} cm). At that time, the left-over disk mass (for an initial ring of $\sim 1 M_\odot$) is about a percent of solar mass, and the outer radius of the disk has expanded to about 10^{14} cm. From that point on, the disk can become easily cooled by photons, and the structure is more likely to resemble an optically thick, geometrically thin disk. With $H/R \sim 0.1$, the viscous timescale becomes now substantially longer, \sim a few $\times 10^8$ s, and the accretion rate declines at a slightly more gentle rate. During this phase of evolution, Cannizzo et al (1990) found that the disk mass, the accretion rate and the outer radius can be approximated by the self-similar solutions

$$M_d(t) = M_d(t_0) \left(\frac{t}{t_0} \right)^{-3/16}, \quad (13)$$

$$\dot{M}_d(t) = \dot{M}_d(t_0) \left(\frac{t}{t_0} \right)^{-19/16}, \quad (14)$$

$$R_d(t) = R_d(t_0) \left(\frac{t}{t_0} \right)^{3/8}, \quad (15)$$

for $t \geq t_0$. Note that, in both the above self-similar solutions, the equation for the disk radius results from the assumptions that most of the disk mass resides in its outermost regions and that the total angular momentum of the disk is conserved. Both these conditions are satisfied in the disk after the fallback phase has ended.

According to the relations above, the disk has the potential to be bright for a very long time. For example, at an age of $\sim 10^5$ yr, such a disk, of mass $\sim 10^{-3} M_\odot$ s^{-1} , would have an accretion rate of about $\sim 10^{14}$ g s^{-1} . The expected luminosities of these disks for ages $\sim 10^4 - 10^5$ yr end up to be in the range of what was discussed for fallback disks around NSs as models to explain the luminosities of the Anomalous X-ray Pulsars (Perna, Hernquist & Narayan 2000). We should also note that the potential for luminous fallback disks left over around BHs after the NS explosion has been discussed by Liu (2003) as a model for Ultraluminous X-Ray Sources.

After the last phase of a geometrically thin, optically thick disk has set in, the following evolution of the gaseous material will depend heavily on the characteristics of the opacity,

and in turn on the metallic content of the material. A detailed discussion of fallback disks from SN explosions (albeit aimed at disks formed around NSs) was presented by Menou et al. (2001b). Their investigation revealed that the power-law evolution continues until a point at which the temperature becomes low enough that the thermal-ionization instability may set in (e.g. Haumery et al. 1998; Menou et al. 2001b). From that point on, the magneto-rotational instability, which provides an important source of viscosity (Balbus & Hawley 1991) may no longer be able to operate, and then the outcome would be that of a 'dead' disk, unable to accrete viscously, and simply cooling. For a solar composition disk, the local stability criterion is (e.g. Hameury et al. 1998)

$$\dot{M}_d(R) > \dot{M}_{\text{crit}}(R) \simeq 9.5 \times 10^{15} m_{10}^{-0.9} R_{10}^{2.68} \text{ g s}^{-1}, \quad (16)$$

where R_{10} is the radius of interest in units of 10^{10} cm. For Helium and metal-dominated disks, one may expect slight deviations from the scaling above (e.g. Menou et al. 2001b). In the case of the disks under consideration here, and strictly adopting Eq. (16), the outermost parts would have become passive up to a radius of $\sim 2 \times 10^{11}$ cm at the time of the transition between the super-Eddington phase described by Eq. (12) and the sub-Eddington one described by Eq. (15). However, we note that Eq.(16) has been derived under the condition of a geometrically thin disk, and hence it should not be applied to the optically thick, hyper Eddington conditions of the early times⁴. Furthermore, even during the early phases of the sub-Eddington phase, when the accretion rate is still relatively high, irradiation of the outer parts of the disk by the X-rays produced in the inner regions of the disk itself (disk self-irradiation) can affect both the time evolution of the accretion rate ($\dot{M}_d \propto t^{-4/3}$ for irradiation-dominated disks; Cannizzo & Gehrels 2009), as well as the critical mass accretion rate below which the disk becomes thermally unstable (Dubus et al. 1999; Menou et al. 2001b; see also Currie & Hansen 2007 for fallback disk evolution with layered accretion).

In the disks under consideration here, the outer parts have had enough time to expand to relatively large radii ($10^{13} - 10^{14}$ cm) during the hyper Eddington phase, when the viscous timescale is very short. Therefore, albeit keeping in mind that the scalings of Eq.(12) are approximate, and that there are many uncertainties in the early hyper Eddington phases (including the likely presence of outflows which are not captured by Eq.(12)), we entertain the possibility that, early on, mass has been transported beyond the radius at which the MRI stops operating when the disk cools at later times.

Among the interesting consequences of a long-lived and extended fallback disk around a BH, is the intriguing possibility of forming planets, which, after the disk has dispersed, would remain in orbit around the BH. Such a scenario was originally proposed by Lin et al. (1991) for the origin of the planets around the radio pulsar PSR 1257+12 (Wolszczan & Frail 1992; Wolszczan 1994), and further investigated by Currie & Hansen (2007). Conditions for planet formation, through phases of grain growth and planetesimal formation,

⁴ The stability properties of hyperaccreting disks have been studied by a number of authors (e.g. Di Matteo et al. 2002; Chen & Beloborodov 2007); due to the very high temperatures, these disks have been found to be stable with respect to the thermal and viscous stability, but possibly gravitationally unstable in the outer regions (see also Perna, Armitage & Zhang 2006). Dead zones due MRI suppression have been identified as a result of the neutrino viscosity in the innermost parts of the disk (Masada et al. 2007). However, these are not of a concern to us, since at accretion rates $\sim 10^{-7} - 10^{-6} M_\odot \text{ s}^{-1}$ the flow is optically thin to neutrinos.

have since been shown to arise in the outer regions of these fallback disks. However, for planets to be able to survive, the disk must extend beyond the tidal disruption radius for a self-gravitating body of density ρ (e.g. Aggarwal & Oberbeck 1974) orbiting an object of mass M

$$R_{\text{tid}} \approx \left(\frac{M}{\rho} \right)^{1/3}. \quad (17)$$

For a BH of $\sim 15 M_{\odot}$, a self-gravitating body of density $\rho \approx 1 \text{ g cm}^{-3}$ has a tidal radius of $\sim 2.5 \times 10^{11} \text{ cm}$, and hence the outer layers of mass which have spread out to $\sim \text{AU}$ distances would allow for the formation and survival of planets.

5. SUMMARY

Fallback disks around newly born compact objects have been invoked to explain a large variety of phenomena. Hyperaccreting disks from the collapse of low-metallicity, rapidly-rotating stars are believed to power long gamma-ray bursts, and have been amply discussed in the literature. In this paper, using the state-of-the-art open source code MESA, we explored the fate of fallback material for 60 stellar models with initial mass in the range $13 - 40 M_{\odot}$, metallicities between 0.01 and $1 Z_{\odot}$ and initial surface rotational velocities between 0.25 and 0.75 of the critical value. Our main focus has been the fate of the high- j fallback material able to circularize and form a disk. By considering a range of explosion energies, we have explored fallback disk formation around both NS and BH remnants. Our 'standard' model included transfer of angular momentum among various layers via magnetic coupling; however, we also explored the evolutionary scenario under the assumption of negligible magnetic torques.

Our main findings are summarized below:

- For strong explosions which leave behind NS remnants, we find that, if magnetic coupling plays an important role during the stellar evolution, the specific angular momentum of the shells immediately outside of the iron core is never large enough for the material to be able to circularize in an orbit outside of the NS radius. Hence fallback disks around newly born NSs are not a common outcome of the SN explosion for strong magnetic coupling.
- If the evolution lacks magnetic coupling among the various layers, a much higher j in the pre-SN star is obtained. In this case, the fallback material does have enough angular momentum to circularize outside the NS radius, even for solar metallicity stars. However, the distribution of the specific angular momentum would require rather fine-tuned conditions in order to produce an extended, long-lived fallback disk. For a very narrow range of explosion energies, a few tens of solar mass of material can fallback and circularize, but just outside the NS surface, hence resulting in a hyperaccreting, highly transient and short-lived disk. Circularization of the outer layers of the envelope at some larger radii would require very special conditions in the explosion geometry: the innermost layers would need to be blown away (or else the NS would quickly turn into a BH), while the outermost layers would need to receive very little of the explosion energy. These special conditions, coupled with the fact that models without magnetic torques are disfavored by observations of the

periods of young pulsars, have led us to conclude that *extended, long-lived fallback disks around isolated NSs are not expected to be a common outcome of supernova explosions.*

- For explosion energies leading to BH remnants, we find that there is always a region in the M, Z, v, E parameter space for which fallback disks are a possible outcome, independently of whether magnetic torques play an important role in the evolution of the star. However, the size of these regions in the parameter space depends on the strength of the magnetic coupling. The explosion material from stars evolved with negligible magnetic torques is able to circularize even for solar-metallicity models with typical initial surface velocities $v_{\text{surf,ini}} \sim 0.2 v_{\text{crit}}$. In the models with strong magnetic coupling, on the other hand, fallback disks are common predominantly at lower metallicities (consistent with what has been found by a number of previous investigations).
- The lower metallicity, faster rotating stars, which lose the outer envelope during their evolution, possess compact fallback disks (circularization occurs within a few tens of Schwarzschild' radii), which result in highly super Eddington accretion rates. The typical fallback time is on the order of a few tens of seconds. The properties of these disks have been widely investigated in the literature as the engines powering long duration Gamma-Ray Bursts, and we have briefly reviewed them here.
- For very weak explosions (or largely anisotropic explosions, with little energy released in the equatorial regions), even the outermost layers of the star can remain bound. In the slower rotating models, for masses $\lesssim 20 M_{\odot}$ and metallicities $\lesssim 0.1 Z_{\odot}$, these outer layers possess a large specific angular momentum. When they fall back, a relatively large mass, $\sim M_{\odot}$, circularizes at a large radius, $\gtrsim 10^3 R_s$. This outcome is common independently of the strength of magnetic torques, as long as the explosion is sufficiently weak or sufficiently asymmetric.

These massive disks around BHs are expected to be long-lived, although the specifics are largely dependent on the properties Z, M, v, B of the main sequence star. For a typical massive star of $M = 13 M_{\odot}$, $v_{\text{surf,ini}} \sim 0.3 v_{\text{crit}}$ and metallicity in the range $Z \sim 1 - 10\% Z_{\odot}$, we find that the outermost $\sim M_{\odot}$ of material falls back on a timescale of several months to $\sim \text{year}$, and circularizes at radii on the order of a few $\times 10^9 - 10^{10} \text{ cm}$ (larger values correlate to lower metallicities of the main sequence star). The initial accretion rate is $\sim 10^{-7} - 10^{-6} M_{\odot} \text{ s}^{-1}$. During the early hyper Eddington phase, when the viscous timescale is very short, these disks can extend to radii on the order of the AU, where tidal forces would not be strong enough to disrupt large gaseous bodies. These disks may harbor the conditions to form planets, hence leading to the possible existence of planets orbiting BHs.

This work was partially supported by NSF grant No. AST 1009396 (RP), NSF grant AST-1009863 (AM) and NSF grant PHY11-25915.

REFERENCES

- Aggarwal, H. R. & Oberbeck, V. R. 1974, *ApJ*, 191, 577
- Alpar, M. A. 2001, *ApJ*, 557L, 61
- Balbus, S. A. & Hawley, J. F. 1991, *ApJ*, 376, 214
- Blackman, E. G. & Perna, R. 2004, *ApJL*, 601, 71
- Braithwaite, J. 2006, *A&A*, 449, 451
- Burrows, A., Hayes, J., Fryxell, B. A. 1995, *ApJ*, 450, 830
- Cannizzo, J. K. 1998, *ApJ*, 494, 366
- Cannizzo, J. K., Lee, H. M. & Goodman, J. 1990, *ApJ*, 351, 38
- Cannizzo, J. K., & Gehrels, N. 2009, *ApJ*, 700, 1047
- Cannizzo, J. K., Troja, E., Lodato, G. 2011, *ApJ*, 742, 32
- Chatterjee, P., Hernquist, L., & Narayan, R. 2000, *ApJ*, 543, 368
- Chen, W.-X., Beloborodov, A. M. 2007, *ApJ*, 657, 383
- Chen, W. C., & Li, X. D. 2006, *A&A*, 450L, 1
- Chevalier, R. A. 1989, *ApJ*, 346, 847
- Chevalier R., Fransson C., 1994, *ApJ*, 420, 268
- Chevalier, R. A., Blondin, J. M., Emmering, R. T. 1992, *ApJ*, 392, 318
- Colgate, S. A. 1971, *ApJ*, 163, 221
- Currie, T. & Hansen, B. 2007, *ApJ*, 666, 1232
- Davidson, K., & Ostriker, J. P. 1973, *ApJ*, 179, 585
- Dexter, J., Kasen, D. 2013, *ApJ*, 772, 30
- D'Angelo, C. R., & Spruit, H. C. 2010, *MNRAS*, 406, 1208
- Di Matteo, T., Perna R., Narayan, R. 2002, *ApJ*, 579, 706
- Duffell, P. C. & MacFadyen, A. I. 2011, *ApJS*, 197, 15
- Duffell, P. C. & MacFadyen, A. I. 2013, arXiv1302.7306
- Dubus, G., Lasota, J.-P., Hameury, J.-M., & Charles, P. 1999, *MNRAS*, 303, 139
- Eksi, K. Y., Hernquist, L., Narayan, R. 2005, *ApJ*, 623L, 41
- Fassia, A., Meikle, W. P. S., Geballe, T. R., et al. 1998, *MNRAS*, 299, 150
- Fendt, C., & Elstner, D. 2000, *A&A*, 363, 208
- Fryer, C., L. & Heger, A. 2000, *ApJ*, 541, 1033
- Fryer, C. L., Herwig, F., Hungerford, A., Timmes, F. X. 2006, *ApJ*, 646L, 131
- Fryxell, B., Arnett, D., Mueller, E. 1991, *ApJ*, 367, 619
- Geng, J. J., Wu, X-F. Huang, Y-F. Yu, Y-B. 20130, preprint arXiv1307.4517
- Giacomazzo, B., Perna, R. 2012, *ApJL*, 758, 8
- Ghosh, P., & Lamb, F. K. 1979, *ApJ*, 234, 296
- Hameury,J.-M., Menou,K., Dubus,G., Lasota, J.-P. & Hureo, J.-M. 1998, *MNRAS*, 298, 1048
- Hayashi, M. R., Shibata, K., & Matsumoto, R. 1996, *ApJ*, 468, L37
- Heger, A., Fryer, C. L., Woosley, S. E., Langer, N., Hartmann, D. H. 2003, *ApJ*, 591, 288
- Heger, A., Woosley, S. E., & Spruit, H. C. 2005, *ApJ*, 626, 350
- Herant, M., Benz, W., Hix, W. R., Fryer, C. L., Colgate, S. A. 1994, *ApJ*, 435, 339
- Hillebrandt, W., & Höflich, P. 1989, *Rep. Prog. Phys.*, 52, 1421
- Ikhsanov, N. R. 2002, *A&A*, 381, L61
- Illarionov, A. F., & Sunyaev, R. A. 1975, *A&A*, 39, 185
- Janiuk, A., Perna, R., Di Matteo, T., Czerny, B. 2004, *MNRAS*, 355, 950
- Janiuk, A., Yuan, Y., Perna, R., Di Matteo, T. 2007, *ApJ*, 664, 1011
- Janiuk, A. & Proga, D. 2008, *ApJ*, 675, 619
- Janka, H.-Th., Langanke, K., Marek, A., Martinez-Pinedo, G., Muller, B. 2007, *Phys. Rep* 442, 381
- Kohri, K., & Mineshige, S. 2002, *ApJ*, 577, 311
- Kohri, K., Narayan, R., & Piran, T. 2005, *ApJ*, 629, 341
- Kotko, I. & Lasota, J.-P. 2012, *A&A*, 545, 115
- Kumar, P., Narayan, R., & Johnson, J. L. 2008, *MNRAS*, 388, 1729
- Langer, N., Fricke, K. J., & Sugimoto, D. 1983, *A&A*, 126, L207
- Levan, A. J. et al. 2013, arXiv1302.2352
- Lee, W. H., Ramirez-Ruiz, E. 2006, *ApJ*, 641, 961
- Lin, D. N. C., Woosley, S. E. & Bodenheimer, P. H. 1991, *Nat.*, 353, 827
- Liu, X-D. 2003, *ApJL*, 596, 199
- Lovelace, R. V. E., Romanova, M. M., & Bisnovaty-Kogan, G. S. 1995, *MNRAS*, 275, 244
- Lovelace, R. V. E., Romanova, M. M., & Bisnovaty-Kogan, G. S. 1999, *ApJ*, 514, 368
- McCray, R. 1993, *ARA&A*, 31, 175
- MacFadyen, A. I. & Woosley, S. E. 1999, *ApJ*, 524, 262
- MacFadyen, A. I. & Woosley, S. E. & Heger, A. 2001, *ApJ*, 550, 410
- Maeder, A. 1987, *A&A*, 173, 247
- Marsden, D. Lingener, R. E. & Rothschild, E. 2001, *ApJ*, 547, L4
- Masada, Y., Kawanaka, N., Sano, T., Shibata, K. 2007, *ApJ*, 663, 437
- Matt, S., Goodson, A. P., Winglee, R. M., & Böhm, K.-H. 2002, *ApJ*, 574, 232
- Menou, K., Hameury, J.-M., Stehle, R. 1999, *MNRAS*, 305, 79
- Menou, K., Perna, R. & Hernquist, L. 2001a, *ApJL*, 554, 63
- Menou, K., Perna, R. & Hernquist, L. 2001b, *ApJ*, 559, 1032
- Metzger, B. D., Piro, A. L., Quataert, E. 2008, *MNRAS*, 390, 781
- Metzger, B. D., Giannios, D., Thompson, T. A., Bucciantini, N., Quataert, E. 2011, *MNRAS*, 413, 2031
- Mazzali, P. A., Walker, E. S., Pian, E., Tanaka, M., Corsi, A., Hattori, T., G.-Y., A. 2013, *MNRAS*, 432, 2463
- Miller, K. A., & Stone, J. M. 1997, *ApJ*, 489, 890
- Michel, F. C. Dressler, A. J. 1981, *ApJ*, 251, 654
- Michel, F. C. 1988, *Nature*, 333, 644
- Mignani, R., et al. 2007, *ApS&S*, 308, 203
- Narayan, R. & Yi, I. 1994, *ApJ*, 428, L13
- Narayan, R. & Yi, I. 1995, *ApJ*, 444, 231
- Narayan, R., Piran, T., & Kumar, P. 2001, *ApJ*, 557, 949
- Nomoto, K., Tominaga, N., Tanaka, M., Maeda, K., Suzuki, T., Deng, J. S., Mazzali, P. A. 2006, *il Nuovo Cim. B* 121, 1207
- Pavlov, G. G., Sanwal, D., & Teter, M. A. 2004, in *IAU Symp. 218, Young Neutron Stars and Their Environments*, ed. F. Camilo & B. M. Gaensler (San Francisco: ASP), 239
- Perna, R., & MacFadyen, A. 2010, *ApJ*, 710L, 103
- Perna, R., Bozzo, E., Stella, L. 2006, *ApJ*, 639, 363
- Perna, R., Hernquist, L., Narayan, R. 2000, *ApJ*, 541, 344
- Perna, R., Armitage, P. J., Zhang, B. 2006, *ApJL*, 636, 29
- Popham, R., Woosley, S. E., & Fryer, C. 1999, *ApJ*, 518, 356
- Piro, A. L. & Ott, C. D. 2011, *ApJ*, 736, 108
- Pringle, J. E. 1974, PhD Thesis, Univ. of Cambridge
- Pringle, J. E. 1991, *MNRAS*, 248, 754
- Rappaport, S. A., Fregeau, J. M., & Spruit, H. 2004, *ApJ*, 606, 436
- Romanova, M. M., Ustyugova, G. V., Koldoba, A. V., & Lovelace, R. V. E. 2004, *ApJ*, 616, L151
- Romanova, M. M., Ustyugova, G. V., Koldoba, A. V., & Lovelace, R. V. E. 2009, *MNRAS*, 399, 1802
- Quataert, E. & Kasen, D. 2012, *MNRAS*, 419L, 1
- Qiao, G. J., Xue, Y. Q., Xu, R. X., Wang, H. G., & Xiao, B. W. 2003, *A&A*, 407, L25
- Shen, R.-F. & Matzner, C. D. 2013, arXiv:1305.5570
- Shakura, N. I., & Sunyaev, R. A. 1973, *A&A*, 24, 337
- Shi, Y., & Xu, R. X. 2003, *ApJL*, 596, 75
- Shibata, M., Sekiguchi, Yu-I., Takahashi, R. 2007, *PTHPh*, 118, 257
- Spyromilio, J. 1991, *MNRAS*, 253, 25
- Spruit, H. C. 2002, *A&A*, 381, 923
- Suijs, M. P. L., Langer, N., Poelarends, A.-J., et al. 2008, *A&A*, 481, L87
- Tassoul, M. 1980, *ApJS*, 43, 469
- Surman, R., McLaughlin, G. C., Hix, W. R. 2006, *ApJ*, 643, 1057
- Thompson, T. A., Chang, P., & Quataert, E. 2004, *ApJ*, 611, 380
- Yan, T., Perna, R., Soria, R. 2012, *MNRAS*, 423, 2451
- Yoon, S.-C., & Langer, N. 2005, *A&A*, 443, 643
- Yoon, S.-C., Langer, N., & Norman, C. 2006, *A&A*, 460, 199
- Wang, Z., Chakrabarty, D., & Kaplan, D. 2006, *Nature*, 440, 772
- Wolszczan, A. 1994, *Science*, 264, 538
- Wolszczan, A., & Frail, D. A. 1992, *Nature*, 355, 145
- Woosley, S. E. 1993, *ApJ*, 405, 273
- Woosley, S. E., & Heger, A. 2012, *ApJ*, 752, 32
- Woosley, S. E., Eastman, R. G., Weaver, T. A., & Pinto, P. A. 1994, *ApJ*, 429, 300
- Woosley, S. E., & Heger, A. 2006, *ApJ*, 637, 914
- Woosley, S. E. & Weaver, T. A. 1995, *ApJS*, 101, 181
- Woosely, S. & Janka, T. 2005, *Nat. Phys.* 1, 147
- Xu, R. X., Wang, H. G., & Qiao, G. J. 2003, *Chinese Phys. Lett.*, 2, 314
- Zahn, J.-P., Brun, A. S., & Mathis, S. 2007, *A&A*, 474, 145
- Zhang, D., & Dai, Z. G. 2008, *ApJ*, 683, 329
- Zhang, D., & Dai, Z. G. 2009, *ApJ*, 703, 461
- Zhang, W., Woosley, S. E. & Heger, A. 2008, *ApJ*, 679, 639
- Zhang, B., Fan, Y. Z., Dyks, J., Kobayashi, S., Meszaros, P., Burrows, D. N., Nousek, J. A., Gehrels, N. 2006, *ApJ*, 642, 354